1-1-2014

Correlation Between the Microstructure and Mechanical Properties of Irradiated Fe-9Cr ODS

M. Swenson
Boise State University

C. Dolph
Boise State University

J. Wharry
Boise State University

Publication Information

Swenson, M.; Dolph, C.; and Wharry, J.. (2014). "Correlation Between the Microstructure and Mechanical Properties of Irradiated Fe-9Cr ODS". *2014 Annual Meeting - Transactions of the American Nuclear Society and Embedded Topical Meeting: Nuclear Fuels and Structural Materials for the Next Generation Nuclear Reactors, NSFM 2014, 110*, 421-424.

Correlation Between the Microstructure and Mechanical Properties of Irradiated Fe-9Cr ODS

M. Swenson[1], C. Dolph[1], J. Wharry[1]

[1] *Boise State University*
1910 University Dr., Boise, ID 83725
matthewswenson1@u.boisestate.edu

INTRODUCTION

The growing global demand for energy will increasingly call upon fusion reactors and Generation IV nuclear fission reactors to supply safe and reliable energy worldwide. Ferritic/martensitic (F/M) alloys are leading candidates for structural components in these reactors because of their high strength, dimensional stability, and low activation. In novel reactor concepts, these materials will be subject to extreme operating conditions, accumulating doses of irradiation up to a few hundred displacements per atom (dpa) at temperatures as high as 600°C. Oxide dispersion strengthened (ODS) F/M alloys containing a dispersion of Y-Ti-O nanoclusters have been developed to operate at even higher temperatures.

The objective of this work is to correlate irradiation-induced microstructural changes, sink strengths, and irradiation-induced hardening in a model Fe-9Cr ODS alloy. A number of recent studies have focused on the phase stability, microstructure evolution, and radiation-induced segregation (RIS) of these alloys. Meanwhile, other efforts have focused on the evolution of ODS mechanical properties under irradiation. However, few studies have combined both microstructural and mechanical analyses to thoroughly understand the irradiation response of these materials.

This work uses self-ion irradiation, nanoindentation, and microscopy to measure the response of Fe-9Cr ODS to irradiation. A thorough literature search identifies sink strength and hardening formulae proposed for each microstructural feature. Experimental measurements are then compared through these formulae to determine expressions that most effectively predict the irradiation response. This work will ultimately aid in understanding the behavior of sinks in irradiated materials.

EXPERIMENTAL DETAILS

Material

A rod of Fe-9Cr ODS material was provided by the Japan Nuclear Cycle Development Institute (now known as the Japan Atomic Energy Agency). The composition is provided in Table I. The rod was heat treated at 1050°C for 1 hour, air cooled, then tempered at 800°C with subsequent air cooling. Electrical discharge machining (EDM) was used to cut the rod into 1.5 mm x 1.5 mm x 20 mm bars. Prior to irradiation, the bar specimens were mechanically polished through 4000 grit SiC paper, followed by electropolishing in a 10% perchloric acid + 90% methanol solution maintained at -30°C.

TABLE I. Chemical Composition of 9-Cr ODS

Chemical Composition (wt%, bal. Fe)							
C	Si	Mn	Ni	Cr	W	Ti	Y
0.14	0.048	0.05	0.06	8.67	1.95	0.23	0.28

Also includes trace amounts of P, S, N, and Ar
[Y2O3] = 1.27 x [Y]
[Ex. O] = [Total O] – [O in Y2O3 powder] = [O] – 0.27 x [Y]

Irradiation

Specimens were irradiated with 5.0 MeV Fe^{++} ions (dose rate ~10^{-3} dpa/sec) using a 1.7 MV General Ionex Tandetron accelerator at the Michigan Ion Beam Laboratory. The accelerator beam line was maintained at pressures below 10^{-7} torr, and the irradiation temperature was maintained at 399.3±4.4°C. Thermocouples and a 2D infrared thermal pyrometer were used for thermal monitoring. Displacement damage was calculated with the Stopping and Range of Ions in Matter (SRIM) program. The damage peak occurs at a depth of 1.2 μm as shown in Fig. 1. All dose measurements and analyses were performed at a depth of 500 ± 100 nm. This depth was selected because it avoids both surface effects and damage/implantation peak effects.

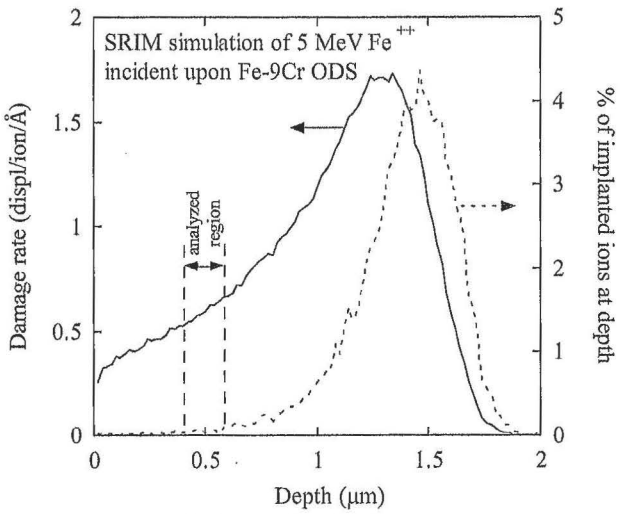

Fig 1. SRIM simulation of 5.0 MeV Fe^{++} ions incident upon Fe-9Cr ODS.

Microscopy

Transmission electron microscopy (TEM) lift-out samples were prepared using an FEI Quanta 3D FEG Focused Ion Beam (FIB). FIB work was carried out at the Environmental Molecular Sciences Laboratory at Pacific Northwest National Laboratory and at the Center for Advanced Energy Studies. The lift-out specimens were oriented perpendicular to the irradiated surface.

Microstructure was characterized using a 200 kV JEOL 2100 TEM at the Boise State Center for Materials Characterization. The following microstructural features were measured: grain and lath dimensions, dislocation line density, precipitate effective diameter and number density, oxide nanoparticle diameter and number density, and dislocation loop diameter and number density (when present). Dislocation loops were imaged "edge-on" using the $\mathbf{g} = 002$ condition for the [001] zone axis, the $\mathbf{g} = -110$ and $\mathbf{g} = 002$ conditions for the [110] zone axis, and the $\mathbf{g} = 01\bar{1}$ condition for the [111] zone axis.

Nanoindentation

Nanoindentation was performed with a Digital Instruments Dimension 3100 SPM that was fitted with a Berkovich Indenter using the Hysitron TS 75 Triboscope located at the Surface Science Laboratory at Boise State University. Displacement-controlled indents were made to depths of 50, 100, 200, 300, and 400 nm on the irradiated Fe-9Cr ODS, but only 200 and 300 nm indents were made on the as-received sample. All indents were performed with a 20 second loading time, a five second hold time, and a 20 second unloading time that accounted for thermal drift and creep. A minimum of 10 indents were performed at each depth for statistical confidence.

RESULTS

Microstructure

All microstructural measurements are provided in Table II for both the as-received and 400°C, 100 dpa conditions. Grain dimensions and dislocation line densities were statistically invariant across both conditions. The most notable differences are the irradiation-induced nucleation of voids and dislocation loops, reduction of oxide nanoparticle size, and increase in nanoparticle density. The size and density of dislocations loops measured are consistent with those found by Yao, et al. [1] in studying an F82H alloy irradiated with neutrons to 3.9 dpa at 400 °C. In addition, studies by Allen, et al. [2] and Certain, et al. [3] conducted on the same heat of this alloy demonstrated similar responses in reduced size and increased density of the nanoparticles upon irradiation.

TABLE II. Microstructure Measurements and Hardening

Feature	Measurement	As Received	400°C, 100 dpa
Grains/Laths	Effective d (10^{-6} m)	0.23	0.28
Dislocation Lines	Density (10^{14} m^{-2})	19.1	20.4
	Stress increase (MPa)	391	404
Carbides	Eff. Diameter (10^{-6} m)	0.11	0.09
	Density (10^{20} m^{-3})	0.20	0.17
	Stress increase (MPa)	92	78
Oxides (Nano-particles)	Diameter (10^{-9} m)	4.29	2.51
	Density (10^{21} m^{-3})	5.5	14.0
	Stress increase (MPa)	302	369
Voids	Diameter (10^{-9} m)	0	7.46
	Density (10^{21} m^{-3})	0	0.46
	Stress increase (MPa)	0	46
Dislocation Loops	Diameter (10^{-9} m)	0	21.5
	Density (10^{21} m^{-3})	0	3.1
	Stress increase (MPa)	0	190
Bulk	Stress increase (MPa)	316	518
Total	Stress increase (MPa)	707	922

Nanohardness

Nanohardness results are shown in Fig. 2. The large confidence intervals for 50 nm, and 100 nm are due to indentation size effects, and implantation and surface effects as described by Hosemann, et al. [4]. An indent depth variation exists for the 400 nm indents due to the load limit of the instrument being exceeded near 400 nm for this material.

When performing a nanoidentation, the plastic deformation zone that is created causes the area that is sampled to be approximately five times the depth of the indent [4]. To ensure that the 400–600 nm range is sampled the ideal indentation depth would be 100 nm. However, sputtering effects (from the irradiation) created a surface roughness on the same order as the 50 and 100 nm indents. On the other hand, the plastic zone created from 300 and 400 nm indents include the irradiation damage and Fe^{++} implantation peaks. Thus, this study will focus on the 200 nm indents since they minimize both surface and implantation effects. The amount of irradiation-induced hardening at 200 nm is 0.90 GPa, as given in Table III.

Studies reported in the literature have shown that the plastic zone decreases as a material's yield strength increases. Due to the high yield strength of ODS steels, it is possible that the plastic zone is <5 times the depth of the indent. As such, it is plausible that a 200 nm indent reasonably measures irradiation hardening in the 500 ± 100 nm region in which microstructure is studied.

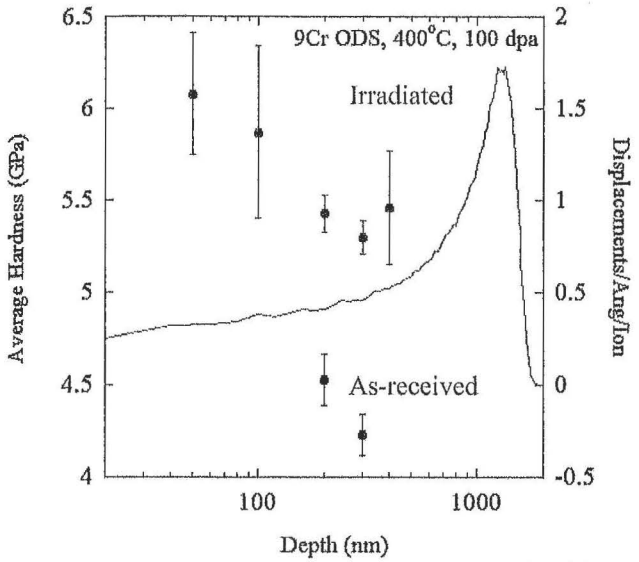

Fig. 2. Nanohardness results on 9% Cr ODS steel, with damage peak superimposed.

TABLE III. Irradiation hardening of 9% Cr ODS steel.

Depth (nm)	H_{avg} (GPa) As Received	H_{avg} (GPa) 400°C, 100 dpa	ΔH_{avg} (GPa)
50	–	6.08	–
100	–	5.87	–
200	4.53	5.43	0.90 ± 0.25
300	4.23	5.3	1.07 ± 0.21
400	–	5.46	–

DISCUSSION

Microstructure-based Strengthening Model

Microstructure can be directly related to macroscopic mechanical properties such as hardness and yield stress through the dispersed barrier hardening model. This model was used to calculate the respective contribution to the yield stress from each microstructural feature observed (dislocations, precipitates, oxide nanoparticles, voids and dislocation loops). Formulations given in Was [5] have been used, and their respective hardness contributions are given in Table II.

The "bulk" strengthening contribution ($\Delta\sigma_{sb}$) of the short-range obstacles was calculated using a superposition model developed by Odette, et al [6] in which a strength factor, S, was introduced as:

$$S = \alpha_s - 5\alpha_w + 3.3\alpha_s\alpha_w \quad (1)$$

where α_s and α_w are defined as the strongest and weakest obstacles, respectively. This factor is then applied to calculate the total bulk stress increase due to obstacles in the matrix ($\Delta\sigma_{sb}$) as a combination of the linear sum ($\Delta\sigma_{ls}$) and the room square sum ($\Delta\sigma_{rs}$) by:

$$(\Delta\sigma_{sb} - \Delta\sigma_{rs}) = S(\Delta\sigma_{ls} - \Delta\sigma_{rs}) \quad (2)$$

in which:

$$\Delta\sigma_{ls} = \Delta\sigma_p + \Delta\sigma_{np} + \Delta\sigma_v + \Delta\sigma_l \quad (3)$$

$$\Delta\sigma_{rs} = \sqrt{\Delta\sigma_p^2 + \Delta\sigma_{np}^2 + \Delta\sigma_v^2 + \Delta\sigma_l^2} \quad (4)$$

Strengthening due to precipitates (p), nanoparticles (np), voids (v) and loops (l) are indicated with subscripts.

The total strengthening of the material ($\Delta\sigma_t$) was calculated by combining the contribution of the dislocation network ($\Delta\sigma_d$) with the bulk strengthening:

$$\Delta\sigma_t = \Delta\sigma_d + \Delta\sigma_{sb} \quad (5)$$

Through this formulation, the measured microstructure can account for 707 MPa of the total yield stress of the as-received specimen, and 922 MPa of the irradiated specimen (Table II). Note that the strengthening contribution of the microstructure, as calculated here, is not considered to be the total yield stress. Factors such as solid solution hardening and lattice friction hardening also contribute to the total yield stress of the material. However, if these factors are assumed to remain constant under irradiation, one can calculate that irradiation-induced microstructural changes can account for 215 MPa increase in yield strength.

Strengthening Model vs. Nanoindentation Results

Hardening measurements (ΔH) from nanoindentation can be converted into a change in yield strength through the following expression [7]:

$$\Delta\sigma_y = 3.06\Delta H \quad (6)$$

Indents to a depth of 200 nm suggested irradiation-induced hardening of 0.90 GPa, which is equivalent to a yield strength increase of 281 MPa. This value is larger than the 215 MPa yield strength increase calculated from the microstructure, but is on the same scale. There also remain other factors to consider in the strengthening model, such as features smaller than the resolution of the TEM, radiation-induced segregation effects, and irradiation-induced oxide nanoparticle dissolution. It has also been noted that 200 nm indents may sample a higher irradiation dose than that in the 500 ± 100 nm region where microstructure was studied.

SUMMARY & FUTURE WORK

A model Fe-9Cr ODS steel was irradiated using 5.0 MeV Fe^{++} ions to 100 dpa at 400°C, which induced the formation of dislocation loops and dissolution of the oxide nanoparticles. Microstructure-based strengthening expressions estimated a change in yield strength of 215 MPa, while nanoindentation measured the change in yield strength to be 281 MPa. This difference is believed to be attributed to experimental limitations in both the microscopy and nanoindentation techniques.

Ongoing work to complete this study involves a thorough survey of all published dispersion hardening model variations. The formulations presented by Was [5] have been used here, but other formulations will be studied to ascertain the most consistency between microstructure and nanohardness measurements. Sink strength formulations will also be investigated in the same manner. This study will ultimately result in a more complete understanding of the behavior of sinks in an irradiated material. This work will enable one to correlate the ability of a sink to attract point defects, with its ability to harden the material.

REFERENCES

1. B. YAO, D. J. EDWARDS, and R. J. KURTZ, "TEM characterization of dislocation loops in irradiated bcc Fe-based steels," *J. Nucl. Mater.*, 434, 402-410 (2013).
2. T. R. ALLEN, J. GAN, J. I. COLE, M. K. MILLER, J. T. BUSBY, S. SHUTTHANANDAN, and S. THEVUTHANSAN, "Radiation response of a 9 chromium oxide dispersion strengthened steel to heavy ion irradiation," *J. Nucl. Mater.*, 375, 26-37 (2008).
3. A. G. CERTAIN, K. G. FIELD, T. R. ALLEN, M. K. MILLER, J. BENTLEY, and J. T. BUSBY, "Response of nanoclusters in a 9Cr ODS steel to 1 dpa, 525°C proton irradiation," *J. Nucl. Mater.*, 407, 2-9 (2010).
4. P. HOSEMANN, D. KIENER, Y. WANG, and S. A. MALOY, "Issues to consider using nano indentation on shallow ion beam irradiated materials," *J. Nucl. Mater.*, 425, 136-139 (2012).
5. G. S. WAS, *Fundamentals of Radiation Materials Science: Metals and Alloys*, pp. 597-606, Springer (2007).
6. G. R. ODETTE and G. E. LUCAS, "Recent progress in understanding reactor pressure vessel steel embrittlement," *Radiat. Eff. Defects Solids*, 144, 189-231 (1998).
7. J. T. BUSBY, M. C. HASH, and G. S. WAS, "The relationship between hardness and yield stress in irradiated austenitic and ferritic steels," *J. Nucl. Mater.*, 336, 267-278 (2005).